European Journal of Neuroscience, pp. 1–10, 2013 doi:10.1111/ejn.12143

Coherent neocortical 40-Hz oscillations are not present during REM sleep

Santiago Castro,[1] Atilio Falconi,[1] Michael H. Chase[2,3] and Pablo Torterolo[1]
[1]Department of Physiology, School of Medicine, Universidad de la República, General Flores 2125, 11800, Montevideo, Uruguay
[2]WebSciences International, Los Angeles, CA, USA
[3]UCLA School of Medicine, Los Angeles, CA, USA

Keywords: cat, consciousness, cortex, EEG, synchronization

Abstract

During cognitive processes there are extensive interactions between various regions of the cerebral cortex. Oscillations in the gamma frequency band (≈40 Hz) of the elecroencephalogram (EEG) are involved in the binding of spatially separated but temporally correlated neural events, which results in a unified perceptual experience. The extent of these interactions can be examined by means of a mathematical algorithm called 'coherence', which reflects the 'strength' of functional interactions between cortical areas. The present study was conducted to analyse EEG coherence in the gamma frequency band of the cat during alert wakefulness (AW), quiet wakefulness (QW), non-rapid eye movement (NREM) sleep and REM sleep. Cats were implanted with electrodes in the frontal, parietal and occipital cortices to monitor EEG activity. Coherence values within the gamma frequency (30–100 Hz) from pairs of EEG recordings were analysed. A large increase in coherence occurred between all cortical regions in the 30–45 Hz frequency band during AW compared with the other behavioral states. As the animal transitioned from AW to QW and from QW to NREM sleep, coherence decreased to a moderate level. Remarkably, there was practically no EEG coherence in the entire gamma band spectrum (30–100 Hz) during REM sleep. We conclude that functional interactions between cortical areas are radically different during sleep compared with wakefulness. The virtual absence of gamma frequency coherence during REM sleep may underlie the unique cognitive processing that occurs during dreams, which is principally a REM sleep-related phenomenon.

Introduction

The brain integrates fragmentary neural events that occur at different times and locations into a unified perceptual experience. Understanding the mechanisms that are responsible for this integration, 'the binding problem', is one of the most important challenges that cognitive neuroscience has to solve (von der Malsburg, 1995; Velik, 2009).

Electroencephalographic (EEG) oscillations in the gamma frequency band (≈ 40 Hz) are involved in the integration or binding of spatially separated, but temporally correlated, neural events; recent studies based on magnetoencephalography and electrocorticography have also reported that gamma band oscillations between 60 and 200 Hz may also play a role in this process (Uhlhaas *et al.*, 2011).

An increase in gamma power typically appears during states/behaviors that are characterized by the active cognitive processing of external percepts or internally generated thoughts and images (Uhlhaas *et al.*, 2009, 2011; Rieder *et al.*, 2010). Gamma activity has been observed during attentive wakefulness not only in humans, but also in animals (Bouyer *et al.*, 1981; Llinas & Ribary, 1993; Tiitinen *et al.*, 1993; Steriade *et al.*, 1996; Maloney *et al.*, 1997). Gamma-band rhythmogenesis is inextricably tied to perisomatic inhibition wherein the key ingredient is $GABA_A$-receptor-mediated inhibition (Buzsaki & Wang, 2012).

The degree of EEG coherence between two cortical regions is believed to reflect the strength of the functional interconnections (re-entries) that occur between them (Edelman & Tononi, 2000; Bullock *et al.*, 2003). Recently, Siegel *et al.* (2012) have proposed that frequency-specific correlated oscillations in distributed cortical networks provide indices, or 'fingerprints', of the network interactions that underlie cognitive processes; measures of the association between brain areas based on such frequency-specific signals are likely to provide more detailed information than corresponding measures based on broadband electrophysiological signals or blood oxygen level-dependent functional magnetic resonance imaging (BOLD-fMRI) signals (Siegel *et al.*, 2012).

Coherent EEG activity in the gamma frequency band increases during different behaviors and cognitive functions in both animals and humans (Bouyer *et al.*, 1981; Bressler *et al.*, 1993; Harle *et al.*, 2004). In addition, gamma activity and gamma coherence between different brain areas have been viewed as a possible neural correlate

Correspondence: Dr P. Torterolo, as above.
E-mail: ptortero@fmed.edu.uy

Received 12 March 2012, revised 19 December 2012, accepted 29 December 2012

of consciousness (Llinas *et al.*, 1998). In this regard, coherence in the gamma frequency band is lost during narcosis (unconsciousness) induced by anesthesia (John, 2002; Mashour, 2006).

Cognitive activities not only occur during wakefulness. Dreams, which occur more prominently during rapid eye movement (REM) sleep, are considered a special kind of cognitive activity or proto-consciousness (Hobson, 2009). REM sleep dreams are characterized by their vividness, single-mindedness, bizarreness and loss of voluntary control over the plot. Attention is unstable and rigidly focused, facts and reality are not checked, violation of physical laws and bizarreness are passively accepted, contextual congruence is distorted and time is altered (Rechtschaffen, 1978; Hobson, 2009; Nir & Tononi, 2010). Interestingly, some authors have suggested that cognition during REM sleep mimics frontal lobe dysfunction (Corsi-Cabrera *et al.*, 2003). In contrast, during deep non-REM (NREM) sleep there is an absence of, or at least a strong reduction in, cognitive functions (Hobson, 2009).

What occurs with respect to coherence in the gamma frequency band during sleep? In a pioneering study utilizing magnetoencephalographic recordings, Llinas & Ribary (1993) found that during REM sleep in humans, as in wakefulness, there is large widespread 40-Hz coherent activity that is charactherized by a fronto-occipital phase shift over the brain (Llinas & Ribary, 1993); however, recent studies have challenged these results (see Discussion). In the present report, we answered the preceding question by studing gamma band coherence among different cortical areas during natural sleep and wakefulness in the cat. Preliminary data have been presented in abstract form (Castro *et al.*, 2010, 2011).

Material and methods

Experimental animals

Four adult cats were used in this study. The animals were obtained from, and determined to be in good health by, the Institutional Animal Care Facility. All of the experimental procedures were conducted in accord with the *Guide for the Care and Use of Laboratory Animals* (8th edition, National Academy Press, Washington DC, 2010) and approved by the Institutional Animal Care Commission (protocol no. 71140-1235-09, School of Medicine, Universidad de la República). All efforts were made to use the minimal number of animals necessary to produce reliable scientific data.

Surgical procedures

Surgical procedures that were employed were similar to those used in previous studies (Torterolo *et al.*, 2002, 2009, 2011b). Accordingly, the animals were chronically implanted with electrodes to monitor the states of sleep and wakefulness. Prior to being anesthetized, each cat was premedicated with xylazine (2.2 mg/kg, i.m.), atropine (0.04 mg/kg, i.m.) and antibiotics (Tribrissen®, 30 mg/kg, i.m.). Anesthesia, which was initially induced with ketamine (15 mg/kg, i.m.), was maintained with a gas mixture of isoflourane in oxygen (1–3%). The head was positioned in a stereotaxic frame and the skull was exposed. In order to record the EEG, stainless steel screw electrodes (1.4 mm diameter) were placed on the surface (above the dura matter) of prefrontal and sensory cortical regions (Fig. 1). To reduce volume conduction, the inter-electrode distance was at least 6 mm (between posterior-parietal and auditory primary cortices); the greatest was 22 mm (between prefrontal and visual primary cortices).

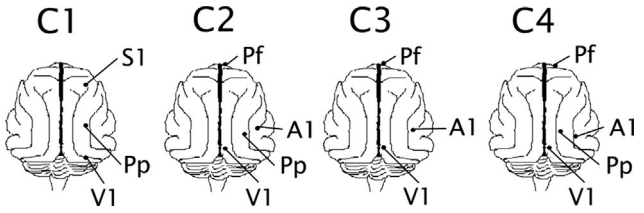

FIG. 1. Position of recording electrodes. The figure depicts the position of the recording electrodes on the surface of the primary sensory, association sensory and prefrontal cerebral cortices. Recordings from these electrodes were referred to a common inactive electrode, which was located over the frontal sinus. The electrodes were located in accordance with previous reports (Thompson *et al.*, 1963; Markowitsch & Pritzel, 1977; Berman & Jones, 1982; Scannell *et al.*, 1995). C1–C4, individual animals. A1, auditory primary cortex; Pf, prefrontal cortex; Pp, posterior-parietal cortex; S1, somato-sensory primary cortex; V1, visual primary cortex.

The electrodes were connected to a Winchester plug, which together with two plastic tubes (which were used to maintain the animal's head fixed without pain or pressure) were bonded to the skull with acrylic cement.

At the end of these surgical procedures an analgesic (Buprenex®, 0.01 mg/kg, i.m.) was administered. Incision margins were kept clean and a topical antibiotic was administered on a daily basis. After the animals had recovered from the preceding surgical procedures, they were adapted to the recording environment for a period of at least 2 weeks.

Experimental sessions

Experimental sessions of 4 h in duration were conducted between 11:00 and 15:00 in a temperature-controlled environment (21–23 °C). All animals had free access to water and food until 1 h prior to the beginning of each recording session. During these sessions (as well as during adaptation sessions), the animal's head was held in a stereotaxic position by four steel bars that were placed into the plastic tubes while the body rested in a sleeping bag (semirestricted condition).

The activity of three cortical areas, from the same cerebral hemisphere, was recorded simultaneously with monopolar electrodes. A common electrode reference montage was employed. The reference electrode was placed in the left frontal sinus; this location is excellent for a common inactive reference electrode, which is critical for the analysis of coherence (Bullock *et al.*, 1995a; Bullock, 1997; Nunez *et al.*, 1997; Cantero *et al.*, 2000). The electromyogram (EMG, of the nuchal muscle which was recorded by means of acutely placed bipolar electrodes) was also monitored. The EMG of the gastrocnemious and temporal muscles, as well as electrocardiogram (EKG) and electrooculogram (EOG, via acutely placed electrodes on the sides of the eyes' orbits) were also recorded in control experiments. Each cat was recorded daily for a period of approximately 30 days in order to obtain complete data sets.

Bioelectric signals were amplified (× 1000), filtered (0.1–100 Hz), sampled (512 Hz, 2^{16} bits) and stored in a PC using Spike 2 software (Cambridge Electronic Design, Cambridge, UK). To discard artifacts in coherence analysis due to digitization of the raw recordings, control experiments were also performed with different combinations of filters (500 Hz highpass filters, with and without a 50-Hz notch filter) as well as with sampling rates of 1024 Hz. No differences were observed in the data obtained in these experiments compared with the data presented in the Results.

Data were obtained during spontaneously occurring quiet wakefulness (QW), REM sleep and NREM sleep. The presence of a

desynchronized EEG and a high level of EMG activity were used to identify wakefulness. NREM sleep was determined by the occurrence of high-amplitude slow waves (0.5–4 Hz) and sleep 'spindles' (9–14 Hz) in the EEG, while REM sleep was identified by a desynchronized EEG with ponto-geniculo-occipital (PGO) waves and atonia (Ursin & Sterman, 1981).

Alert wakefulness (AW) was induced for a period of 300 s by a sound stimulus, which was introduced approximately 30 min after the beginning of the recording. The sound stimulus consisted of clicks (0.1 ms in duration) of 60–100 dB SPL in intensity with a variable frequency of presentation (1–500 Hz, modified at random by the operator) in order to avoid habituation (Torterolo *et al.*, 2003, 2011a). In selected experiments, AW was also induced either by the presentation of a moving light or by placing a mirror in front of the cat. Because the state of alertness always outlasted the duration of the stimulus, a waking state was considered as QW when there was a relatively low EMG and EOG activity several minutes after stimulation.

Data analysis

Sleep and waking states were determined for 10-s epochs. To analyse coherence between pairs of EEG channels, 12 artifact-free periods of 100 s were examined during each behavioral state (1200 s for each behavioral state). For each pair of recordings, data were obtained during four recording sessions.

For each 100-s period, the magnitude squared coherence was analysed as follows – $coh_{ab}\ (f) = [\sum csd_{ab}\ (f)]^2/[\sum psd_a\ (f)\ \sum psd_b\ (f)]$, where psd is the power spectral density, and a and b are the waves that were analyzed. csd, which is the cross spectra density or the Fourier analysis of the cross covariance function, provides a reflection of how common activity between two processes is distributed across frequencies. Coherence between two waveforms is a function of frequency and ranges from 0 for totally incoherent waveforms to 1 for maximal coherence. In order for two waveforms to be completely coherent at a particular frequency over a given time range, the phase shift between the waveforms must be constant and the amplitudes of the waves must have a constant ratio. This mathematical approach was described in detail by Bullock & McClune (1989) and has been validated by several investigators (Bouyer *et al.*, 1981; Bullock & McClune, 1989; Bullock *et al.*, 1995b; Achermann & Borbely, 1998a,b; Cantero *et al.*, 2004).

Magnitude squared coherence was measured using the Spike 2 script COHER 1S (Cambridge Electronic Design). With this algorithm we analysed the coherence between two EEG channels that were recorded simultaneously during 100-s periods. This period of analysis was divided into 100 time-blocks for a sample rate of 512 Hz, with a bin size of 1024 samples and a resolution of 0.5 Hz.

In pilot recordings and analyses, we determined that the level of coherence between cortical leads and EMG recordings (neck, gastrocnemious or temporal), the EKG or the EOG, was approximately 0.1 (Fig. S1).

In this report, we concentrated on examining the coherence of the EEG in the gamma frequency band (30–45 Hz), as originally described by Jasper & Andrews (1938); this narrow band corresponds to the 40-Hz cognitive rhythm introduced by Das & Gastaut (1955). We chose this narrow band of the gamma spectrum for analysis because in preliminary studies we observed that when an animal is alerted by different means, there is a noticeable peak in coherence in this frequency (see Fig. 6). Although some data suggest a role in cognitive functions of higher gamma (60–100 Hz) oscillations, the mechanisms and functions are not clear (Uhlhaas *et al.*, 2011). Nevertheless, we also examined 60–100 Hz oscillations with the aim of determining if some of the observed phenomena extend to higher frequencies.

To normalize the data and evaluate them by means of parametric statistical tests, we applied the Fisher z′ transform to the gamma coherence values. Thereafter, the profile of the z′-coherence of the gamma band in 100-s epochs for each pair of EEG recordings, as well as the average of 12 epochs, was analysed; the results were presented in graphic form (see Figs 6–8). The z′-coherence of the gamma band for each pair of EEG channels, which was also averaged across behavioral states independently for each cat, was expressed as the mean ± standard error. The significance of the differences among behavioral states was evaluated with ANOVA and Tamhane *post-hoc* tests. The criterion used to reject the null hypotheses was $P < 0.05$.

Selected recordings were filtered (band pass 35–45 Hz) using Spike 2 digital finite impulse response filters. The amplitude of simultaneously recorded pairs of filtered EEG signals was also analysed by means of the Pearson correlation. Autocorrelations and cross-correlation functions were also performed.

Results

Raw and filtered (30–45 Hz) EEG recordings during AW and REM sleep

The EEG fluctuates from a desynchronized pattern of activity during wakefulness and REM sleep to synchronized activity during NREM sleep. Although EEG activity during wakefulness and REM sleep is similar, there are subtle but striking differences. Representative EEG recordings (prefrontal and posterior parietal leads) are shown in Figs 2 and 3. 'Bursts' of 35–40 Hz oscillations can be readily observed in raw recordings during AW (Fig. 2); in contrast, these electrographic events are difficult to find during REM sleep (Fig. 3). These oscillations were unmasked after digital filtering of the recordings to include only 30–45 Hz activity (Figs 2 and 3). During AW, the 'bursts' of gamma oscillations exhibited spindle morphology with an amplitude and duration of approximately 25 μV and 200–500 ms, respectively. These gamma oscillations during AW, which are clearly observed in the autocorrelation histogram, are accompanied by high values of gamma band power (Fig. 4). In contrast, during REM sleep the amplitude and duration of these events are drastically reduced (Figs 3 and 4).

A strong coupling of EEG signals recorded in different cortical sites was present during AW, but not during REM sleep (Figs 2–4). This high level of coupling between EEG oscillations can be observed in filtered recordings. Coupling is highlighted when the amplitudes of the signals between pairs of simultaneous EEG recordings are correlated. During AW, there was a high correlation between both EEG signals, which was absent during REM sleep (Figs 2–4).

A visual form to represent the increase in gamma power as well as the coupling among different cortices during AW is shown in Fig. 5. Compared with AW, during REM sleep, gamma power was reduced and coupling was not present. However, note that gamma band power during REM sleep is similar to QW and larger than NREM sleep.

Coherent 30–45 Hz activity is present during wakefulness but not during REM sleep

In spite of the fact that EEG coupling was not present during REM sleep when analysed by filtered recordings and correlation methods,

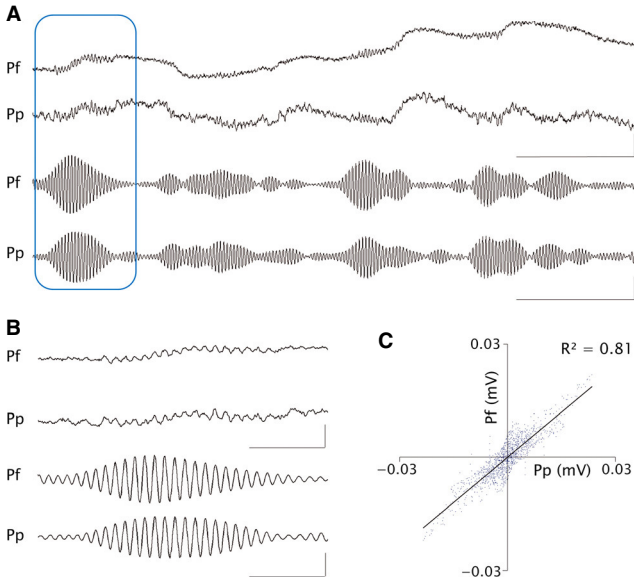

FIG. 2. Gamma oscillations during alert wakefulness. (A) Simultaneous raw and filtered (35–40 Hz) cortical recordings from the prefrontal (Pf) and posterior-parietal cortices (Pp) during alert wakefulness. Gamma oscillations, which are readily observed in the raw recordings, are highlighted after filtering. Scale bars – 1 s and 200 μV for raw recordings and 20 μV for filtered recordings. (B) Gamma oscillations enclosed in A are presented with a longer calibration time. Scale bars – 0.2 s, voltage calibration as in A. (C) Regression and correlation coefficient between the amplitudes of Pf and Pp were analysed from representative filtered recordings during 6 s of alert wakefulness. Regression line equation – $y = 0.8x + 2^{-5}$.

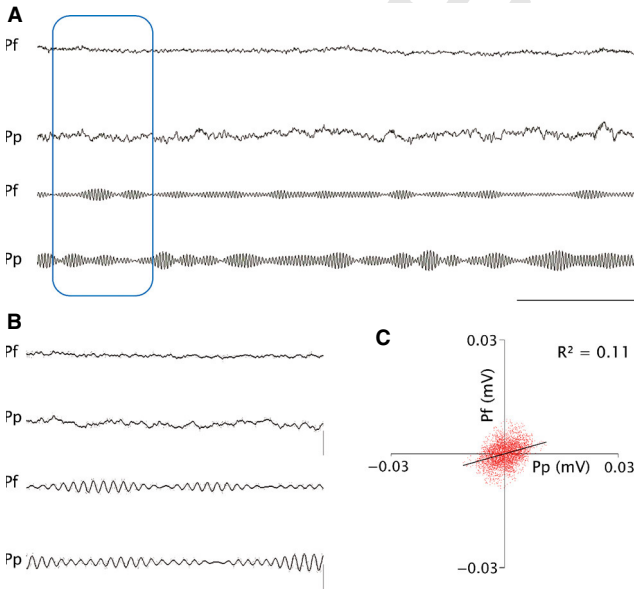

FIG. 3. Gamma oscillations during REM sleep. (A) Simultaneous raw and filtered (35–40 Hz) cortical recordings from the prefrontal (Pf) and posterior-parietal cortices (Pp) during REM sleep. The amplitude and duration of gamma oscillations decreased compared with alert wakefulness (see Fig. 2). Scale bars – 1 s and 200 μV for raw recordings and 20 μV for filtered recordings. (B) Gamma oscillations enclosed in A are shown with a longer calibration time. Scale bars – 0.2 s, voltage calibration as in A. (C) Regression and correlation coefficient between the amplitudes of Pf and Pp were analysed from representative filtered recordings during 6 s of REM sleep. Regression line equation – $y = 0.28x + 2^{-6}$.

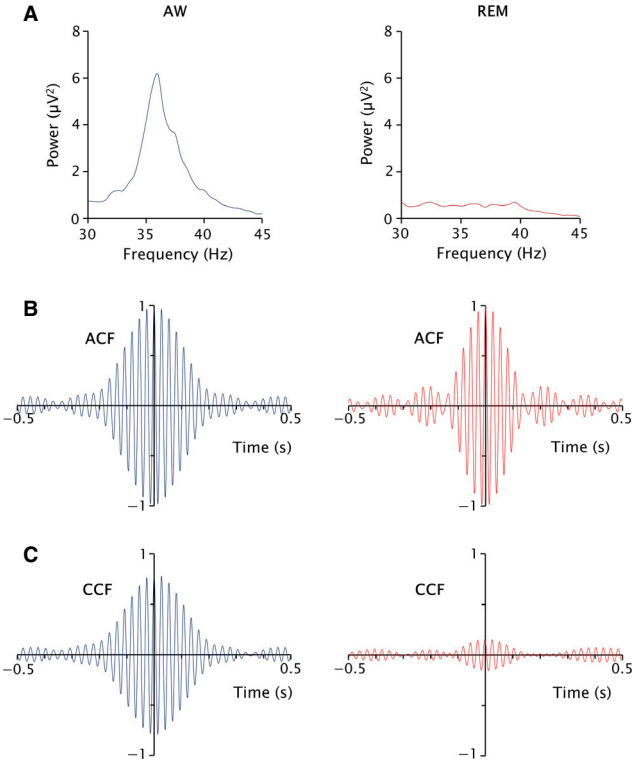

FIG. 4. Gamma oscillations during alert wakefulness (AW) and REM sleep. (A) Gamma band power during AW (left) and REM sleep (right), of the EEG recorded from the prefrontal cortex (100-s window). (B) Autocorrelation function (ACF) from filtered (35–40 Hz) 300-s EEG recordings from the prefrontal cortex during AW (left) and REM sleep (right). (C) Cross-correlation function (CCF) from filtered (35–40 Hz) 300 s of simultaneous EEG recordings from the prefrontal cortex and posterior parietal cortex during AW (left) and REM sleep (right).

we applied the 'coherence' algorithm for an in-depth analysis of different pairs of EEG signals that were simultaneously recorded during wakefulness and sleep.

In pilot studies we analysed the EEG coherence from 0.5 up to 100 Hz (Fig. 6). It is readily observed that when an animal is alerted by different means, there is a clear increase in coherence between 30 and 45 Hz, with a narrow peak between 35 and 40 Hz; hence, this band was selected for further analysis.

z′-Coherence profiles for representative pairs of EEG leads are shown in Fig. 7; the profile of 12 100-s periods and their average for each behavioral state are shown. It is readily observed that z′-coherence profiles for all of the 100-s periods, as well as the average, were larger during AW, with a restricted peak at 35–40 Hz. The z′-coherence decreased during QW and NREM sleep, and was virtually absent during REM sleep.

Examples of the averaged gamma (30–45 Hz) band z′-coherence profiles for different combination of EEG recordings are shown in Fig. 8. For these cortical combinations, the z′-coherence was larger during AW and was drastically reduced during REM sleep. Note that in Fig. 8A, the results of three different procedures for the induction of AW (sound, moving light or exposure to a mirror) were included; the results of these procedures were similar. During AW, the z′-coherence peak reached values up to 2.1, which corresponds to a coherence of 0.97.

The averaged z′-coherence in the 35–40 Hz band across behavioral states for all combinations of cortical recordings is presented in Table 1. In these 15 independent analyses, the results were consis-

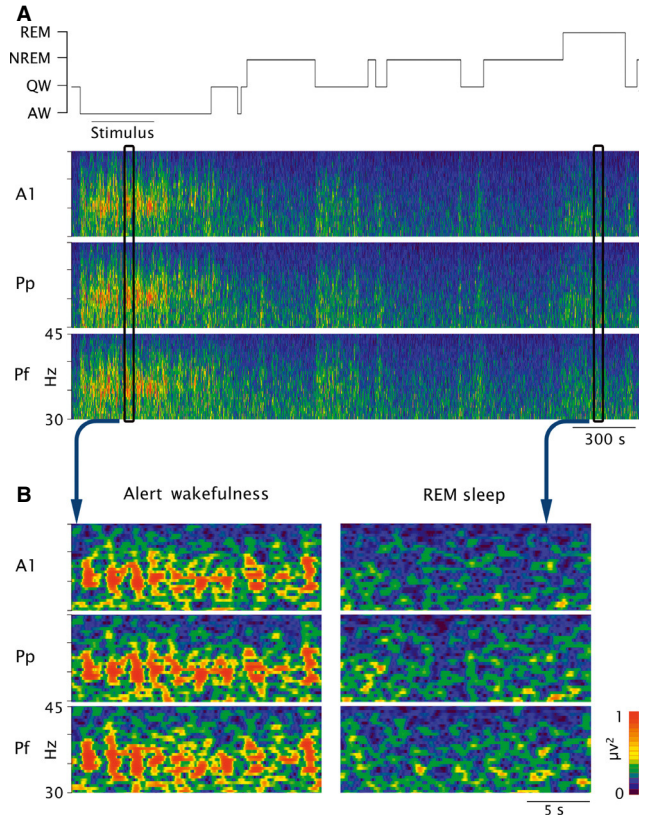

FIG. 5. Gamma band power during alert wakefulness and REM sleep. (A) Hypnogram and simultaneous gamma power spectrogram from EEG recordings of the primary auditory (A1), posterior parietal (Pp) and prefrontal cortices (Pf). During alert wakefulness, gamma power values are larger and more coupled between the recorded cortices than during other behavioral states. A bar under the hypnogram indicates the time of sound stimulation. (B) Twenty-second windows of alert wakefulness and REM sleep. The dynamic of gamma power during alert wakefulness was very similar in the cortices that were simultaneously recorded; this fact was not evident during REM sleep.

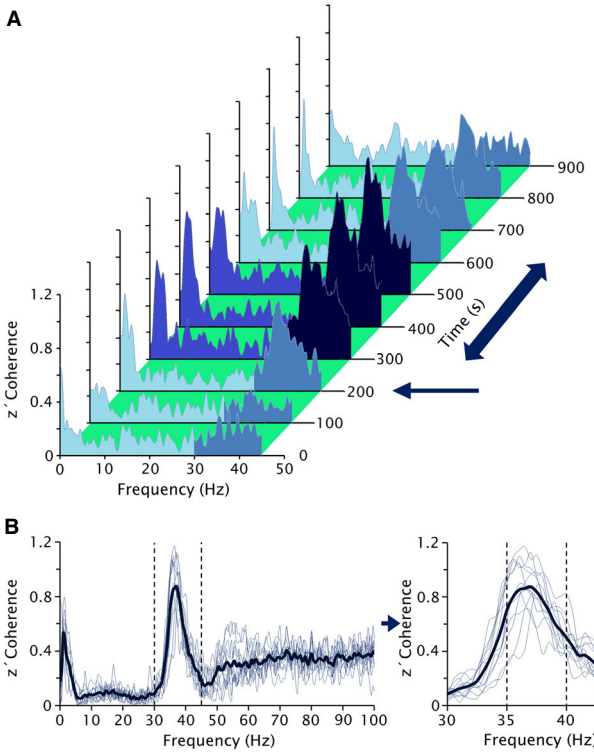

FIG. 6. Profile of EEG coherence during wakefulness. (A) z′-Coherence spectra (0–45 Hz) between the EEG recorded from prefrontal and posterior parietal cortices (1000 s in 100-s epochs). The thin arrow indicates the moment when the experimenter entered the recording room; the thick double-headed arrow indicates the time when sound stimulation was applied. When the animal was alerted by a novel stimulus, there was a clear peak in gamma (30–45 Hz) coherence. The increase in gamma coherence outlasted the sound stimulation. (B) Twelve z′-coherence profiles (thin lines), from a representative pair of recordings (prefrontal and posterior-parietal cortices) during alert wakefulness. The average of these profiles (thick line) is also shown. The profiles were constructed from periods of 100 s, during sound stimulation, with a resolution of 0.5 Hz. The coherence for the gamma band (30–45 Hz) is highlighted to the right.

tent. During AW, there was a significant increase in z′-coherence in most of the combinations, while during REM sleep there was a significant decrease in this parameter. During QW and NREM sleep, z′-coherence values were intermediate, and in several combinations they were larger during QW than during NREM sleep. Differences in the extent of coherence between different recording pairs during the same behavioral state could be related to either the distance between the electrodes and/or the degree of reciprocal connections between them (Cantero *et al.*, 2000).

The z′-coherence, normalized to AW values, highlights the differences between wakefulness and REM sleep (Fig. 9). Depending on the pair of cortical areas analysed, z′-coherence during REM sleep ranged from 60 to 2.6% of the AW values.

Coherence in high (60–100 Hz) gamma band during sleep and wakefulness

Figure 6B shows EEG coherence from 0.5 to 100 Hz during AW. A coherence peak in the 30–45 Hz band occurs during AW; this phenomenon is not observed at higher frequencies.

The dynamic evolution of EEG coherence in high gamma during wakefulness and sleep is shown in Fig. 10. While changes in z′-coherence during AW, QW and NREM sleep were subtle, z′-coherence was drastically reduced during REM sleep (Fig. 10). As shown in Table 2, a significant decrease in z′-coherence during REM sleep occurred in all cortical combinations that were analysed.

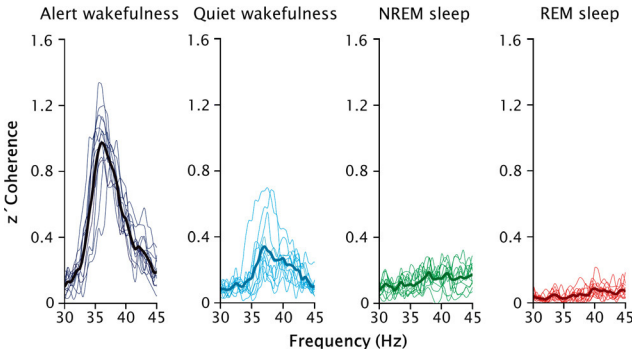

FIG. 7. Profile of EEG gamma (30–45 Hz) coherence during wakefulness and sleep. Twelve profiles of z′-coherences (thin lines) of a representative pair of recordings (prefrontal and posterior-parietal cortices) as well as the averages of these 12 profiles (thick lines) are shown for alert and quiet wakefulness, NREM and REM sleep. The profiles were constructed from periods of 100 s with a resolution of 0.5 Hz. Gamma coherence was maximal during alert wakefulness and practically absent during REM sleep.

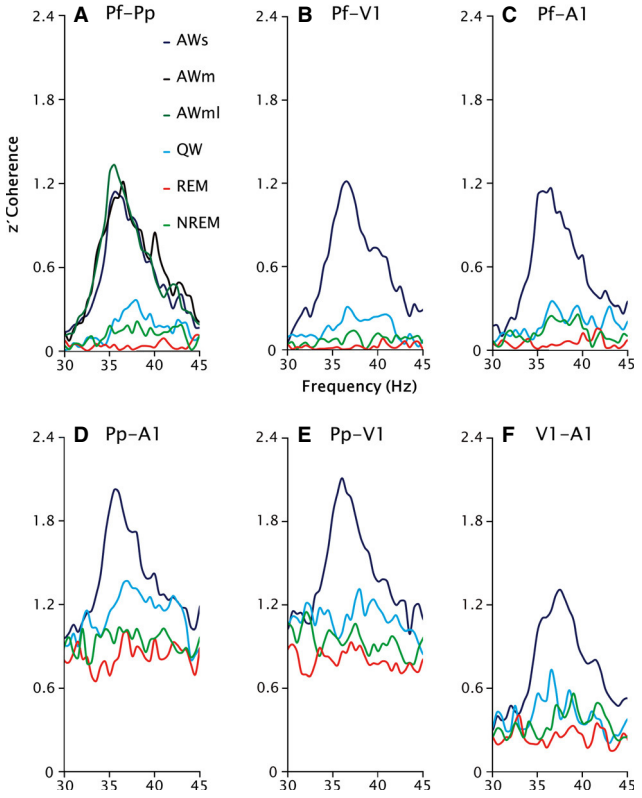

FIG. 8. Gamma band z′-coherence profiles from representative prefrontal-perceptual and perceptual regions during sleep and wakefulness. Graphics at the top (A–C) show z′-coherence between prefrontal and perceptual cortices. At the bottom (D–F), z′-coherences profiles between perceptual cortices are shown. In A, three types of stimuli produced alert wakefulness – sound (AWs), mirror (AWm) and moving light (AWml). In B–F, alertness was produced only by sound stimulation. For all combinations of recordings, z′-coherence in the gamma band was larger during AW than during REM sleep. QW, quiet wakefulness; NREM, non-REM sleep; REM, REM sleep; A1, auditory cortex; Pf, prefrontal cortex; Pp, posterior-parietal cortex; V1, visual primary cortex.

Figure 10C presents 60–100 Hz power spectrum profiles from representative 100-s time epochs. In comparison to AW or QW, high gamma power is reduced during NREM sleep. Note that even though high gamma coherence is reduced during REM sleep (Fig. 10A), high gamma power is similar than waking levels.

Discussion

In the present study, we demonstrated that the EEG intra-hemispheric coherence in the gamma (30–45 Hz) frequency band is larger during AW than during QW. In addition, gamma coherence decreased to a lower level during NREM sleep, and was absent during REM sleep; the lack of coherence during REM sleep also extended to high gamma (60–100 Hz) band frequencies. Therefore, during REM sleep, the coupling of high-frequency neuronal activity among different cortical regions is practically non-existent.

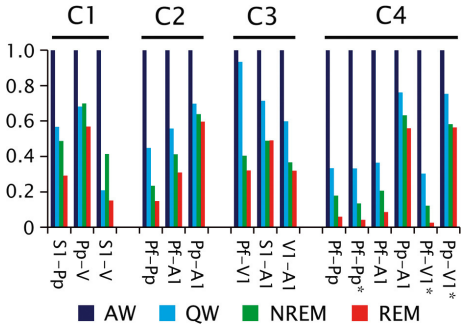

FIG. 9. Gamma band (35–40 Hz) z′-coherence for all analysed cortical combinations. The data from Table 1 were normalized to the values obtained during alert wakefulness. C1–C4, individual animals. A1, auditory cortex; Pf, prefrontal cortex; Pp, posterior-parietal cortex; S1, somato-sensory primary cortex; V1, visual primary cortex. In the derivatives indicated by an asterisk, AW was produced by light stimulation. AW, alert wakefulness; QW, quiet wakefulness; NREM, non-REM sleep; REM, REM sleep.

TABLE 1. Gamma (35–40 Hz) z'-coherence values during sleep and wakefulness

Animal	Derivates	AW	QW	NREM	REM	Statistical significance	*F*
C1	S1-Pp	1.09 ± 0.05	0.62 ± 0.06	0.53 ± 0.04	0.32 ± 0.01	AW vs. all‡; REM vs. QW and NREM†	54
	Pp-V1	1.31 ± 0.06	0.89 ± 0.06	0.92 ± 0.06	0.75 ± 0.06	AW vs. all‡; REM vs. QW and NREM†	46
	S1-V1	0.70 ± 0.05	0.15 ± 0.01	0.29 ± 0.04	0.11 ± 0.01	AW vs. all‡; REM vs. NREM†; NREM vs. QW†	54
C2	Pf-Pp	0.67 ± 0.02	0.30 ± 0.04	0.16 ± 0.01	0.10 ± 0.01	AW vs. all‡; REM vs. QW and NREM†; NREM vs. QW†	114
	Pf-A1	0.87 ± 0.05	0.49 ± 0.03	0.36 ± 0.01	0.27 ± 0.01	AW vs. all‡; REM vs. QW and NREM†	86
	Pp-A1	1.27 ± 0.04	0.89 ± 0.05	0.81 ± 0.01	0.76 ± 0.01	AW vs. all‡; REM vs. QW and NREM†	29
C3	Pf-V1	0.14 ± 0.01	0.13 ± 0.02	0.06 ± 0.01	0.05 ± 0.01	AW vs. REM and NREM†; REM vs. QW†; NREM vs. QW†	18
	S1-A1	0.99 ± 0.02	0.70 ± 0.03	0.48 ± 0.01	0.48 ± 0.01	AW vs. all‡; REM vs. QW†; NREM vs. QW†	137
	V1-A1	0.76 ± 0.02	0.46 ± 0.03	0.28 ± 0.01	0.24 ± 0.03	AW vs. all‡; REM vs. QW†; NREM vs. QW‡	102
C4	Pf-Pp	0.80 ± 0.05	0.27 ± 0.04	0.14 ± 0.01	0.05 ± 0.01	AW vs. all‡; REM vs. QW and NREM‡	118
	Pf-Pp*	0.94 ± 0.03	0.31 ± 0.02	0.13 ± 0.01	0.04 ± 0.00	AW vs. all‡; REM vs. all‡; NREM vs. AW and REM‡	121
	Pf-A1	0.79 ± 0.04	0.29 ± 0.04	0.16 ± 0.01	0.07 ± 0.01	AW vs. all‡; REM vs. QW and NREM‡; NREM vs. QW†	173
	Pp-A1	1.57 ± 0.03	1.20 ± 0.03	0.99 ± 0.02	0.88 ± 0.01	AW vs. all‡; REM vs. QW and NREM‡; NREM vs. QW‡	515
	Pf-V1*	0.86 ± 0.02	0.26 ± 0.02	0.10 ± 0.00	0.02 ± 0.00	AW vs. all‡; REM vs. QW‡; NREM vs. QW‡	616
	Pp-V1*	1.70 ± 0.02	1.28 ± 0.03	0.99 ± 0.02	0.96 ± 0.02	AW vs. all‡; REM vs. QW and NREM‡; NREM vs. QW‡	235

ANOVA with Tamhane tests. The degrees of freedom were 3 (between groups) and 44 (within groups) for all the derivates that were analysed. A1, auditory cortex; Pf, prefrontal cortex; Pp, posterior-parietal cortex; S1, somato-sensory primary cortex; V1, visual primary cortex. AW, alert wakefulness; QW, quiet wakefulness; NREM, non-REM sleep; REM, REM sleep. *In these cortical pairs AW was induced by light stimulation. The values represent mean ± standard error. †$P < 0.05$ and ‡$P < 0.0001$.

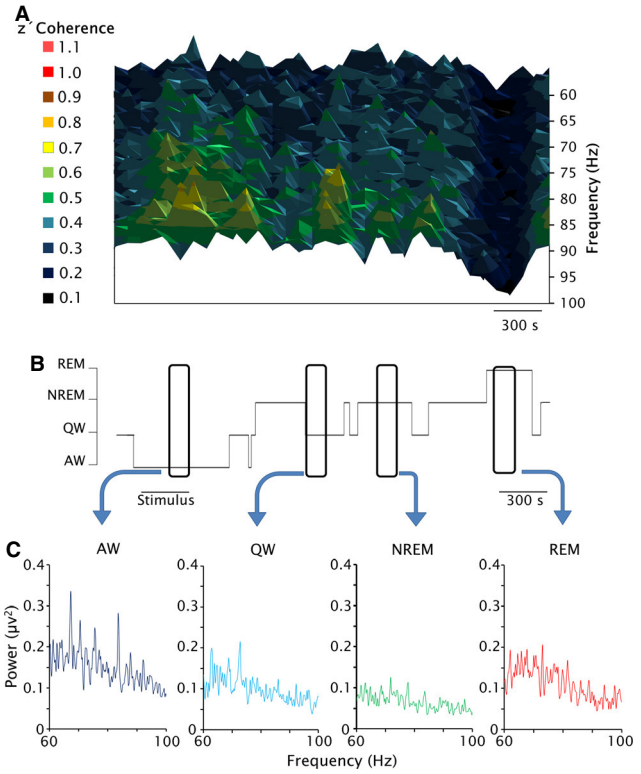

FIG. 10. Dynamic evolution of EEG coherence during sleep and wakefulness. (A) Three-dimensional spectrogram of z′-coherence of the EEG (60–100 Hz) from simultaneous recordings from prefrontal and posterior parietal cortices (3300 s). Time and frequency are shown on the horizontal and vertical (depth) axes, respectively, while z′-coherence is represented in a color code. z′-Coherence is drastically reduced during REM sleep. (B) Hypnogram of recordings analysed in A. The bar under the hypnogram indicates the time of sound stimulation. (C) Gamma band power spectrum profiles from representative 100-s time epochs enclosed in B during AW, QW, NREM sleep and REM sleep.

Animal model

We used the cat as an animal model because it has well-defined, consolidated sleep and waking states. In addition, there are data that suggest that complex, dream-like, cognitive processes are present during REM sleep in this species (Sastre & Jouvet, 1979; Morrison, 1983). Experimental lesions targeted to the dorsal pontine reticular formation elicit REM sleep without atonia; in this condition, dream-like behaviors with complex motor activities, such as jumps and predation-like movements, are released (Sastre & Jouvet, 1979; Morrison, 1983). Furthermore, cortical development is greater in the cat than in rodents, especially in associative cortices; consequently, the cat is an special attractive species in which to study cognitive processes (Thompson *et al.*, 1963; Markowitsch & Pritzel, 1977; Fuster, 1989; Scannell *et al.*, 1995).

Recordings were carried out in semirestricted condition. The advantage is that the differences among states are the states *per se*; changes in postures or movements did not influence the recordings, reducing the possibility of artifacts.

Extra-cerebral potentials did not explain gamma band coherence

There are two main arguments against the possibility that extra-cerebral potentials generated by muscles, heart or eye movements could produce the large 'coherence' observed during AW. First, gamma coherence between the EEG and the activity of different muscles EMGs, EKG or EOG recorded by means of either bipolar or monopolar electrodes was negligible (a portion of these results are shown in Fig. S1). Second, there was a variable latency between most of the peaks of the gamma waves between the different cortices that were recorded simultaneously. This latency was proportional to the distance between the recorded cortices (not shown); it would not be present if the potentials were produced from an extra-cerebral source. This fact also allows one to reject the volume conduction as an important component of gamma band coherence in the present study.

TABLE 2. Gamma (60–100 Hz) z'-coherence values during sleep and wakefulness

Animal	Derivates	AW	QW	NREM	REM	Statistical significance	*F*
C1	S1-Pp	0.63 ± 0.02	0.53 ± 0.01	0.40 ± 0.02	0.19 ± 0.01	REM vs. all‡; AW vs. QW and NREM†	149
	Pp-V1	0.83 ± 0.01	0.76 ± 0.01	0.61 ± 0.02	0.48 ± 0.01	REM vs. all‡; AW vs. NREM‡	122
	S1-V1	0.40 ± 0.01	0.35 ± 0.01	0.21 ± 0.01	0.04 ± 0.01	REM vs. all†; AW vs. QW and NREM†	175
C2	Pf-Pp	0.43 ± 0.01	0.34 ± 0.03	0.31 ± 0.01	0.12 ± 0.01	REM vs. all‡; AW vs. QW and NREM†	58
	Pf-A1	0.51 ± 0.01	0.45 ± 0.02	0.45 ± 0.01	0.25 ± 0.01	REM vs. all‡; AW vs. NREM†	70
	Pp-A1	0.98 ± 0.04	0.86 ± 0.05	0.88 ± 0.02	0.71 ± 0.01	REM vs. all†	10
C3	Pf-V1	0.08 ± 0.00	0.08 ± 0.00	0.05 ± 0.01	0.02 ± 0.00	REM vs. all†; NREM vs. AW and QW†	48
	S1-A1	0.61 ± 0.01	0.43 ± 0.01	0.36 ± 0.02	0.30 ± 0.01	REM vs. all‡; AW vs. QW and NREM†; QW vs. NREM†	46
	V1-A1	0.39 ± 0.02	0.36 ± 0.01	0.18 ± 0.02	0.12 ± 0.02	REM vs. AW and QW‡; NREM vs. AW and QW†	93
C4	Pf-Pp	0.35 ± 0.02	0.31 ± 0.01	0.31 ± 0.03	0.07 ± 0.01	REM vs. all‡	53
	Pf-Pp*	0.37 ± 0.02	0.30 ± 0.02	0.26 ± 0.02	0.03 ± 0.00	REM vs. all‡	110
	Pf-A1	0.31 ± 0.01	0.27 ± 0.01	0.28 ± 0.03	0.07 ± 0.01	REM vs. all†	49
	Pp-A1	0.92 ± 0.02	0.89 ± 0.01	0.85 ± 0.04	0.64 ± 0.05	REM vs. all‡; AW vs. QW and NREM†	16
	Pf-V1*	1.07 ± 0.02	1.11 ± 0.02	0.93 ± 0.02	0.70 ± 0.01	REM vs. all‡; QW vs. NREM†	100
	Pp-V1*	0.45 ± 0.02	0.37 ± 0.02	0.31 ± 0.00	0.06 ± 0.02	REM vs. all‡; AW vs. NREM†	113

ANOVA with Tamhane tests. The degrees of freedom were 3 (between groups) and 44 (within groups) for all the derivates that were analysed. A1, auditory cortex; Pf, prefrontal cortex; Pp, posterior-parietal cortex; S1, somato-sensory primary cortex; V1, visual primary cortex. AW, alert wakefulness; QW, quiet wakefulness; NREM, non-REM sleep; REM, REM sleep. *In these cortical pairs AW was induced by light stimulation. The values represent mean ± standard error. $^{\dagger}P < 0.05$ and $^{\ddagger}P < 0.0001$.

Data in humans indicate that saccadic eye movements can be a source of gamma wave oscillations in frontal derivations (Yuval-Greenberg *et al.*, 2008). In addition to the lack of coherence between the EEG and the EOG, the absence of gamma coherence during REM sleep, when saccadic eye movements predominate, indicates that these movements did not play a role in the generation of gamma coherence in the cat.

Coherence analysis in a 100-s window

To determine general trends in coherence analyses, we employed time windows of 100 s, although the timescale for functionally significant events and fluctuations in the brain is much shorter. In relation to cognitive functions, Libet *et al.* (1991) demonstrated that appropriate neuronal activation of approximately 500 ms in duration is required to elicit a conscious sensory experience (Libet *et al.*, 1991). Therefore, from an electrophysiological point of view, in 100-s time-windows one can average the results of different EEG events that occur during wakefulness (i.e. sensory or motor-evoked events), during NREM sleep (i.e. spindles and slow waves) or REM sleep (i.e. PGO waves and tonic EEG desychronization). Nevertheless, an increase in gamma coupling was also evident during shorter periods of analysis. Good correlation ($R^2 = 0.81$) was evident in filtered recordings during 6-s epochs of AW. Furthermore, coupling was readily observed in the 200–500 ms gamma 'bursts' that were present in the raw and filtered recordings during AW; these synchronized gamma 'bursts' are also identified by their power in Fig. 5 (see also the cross correlation function in Fig. 4). In contrast, gamma band coupling disappeared during REM sleep (Figs 3–5).

Gamma coherence during wakefulness

It is well known that gamma power and gamma coherence increase during wakefulness in animals and humans (Llinas & Ribary, 1993; Maloney *et al.*, 1997; Rieder *et al.*, 2010). In the cat, gamma band coherence increases during AW between electrodes located in cortical and thalamic sites (Bouyer *et al.*, 1981). In accordance with these results, we demonstrated that during AW, coherence increases between different cortical areas; this fact was clearly observed at frequencies of $\approx$ 40 Hz, but not at higher gamma bands. This increase in coherence occurs during alert behaviors that were induced either by sound, moving light stimulation or when a mirror was located in front of the animal (or immediately after these procedures, as shown in Fig. 6). Coherence also increased when the level of alertness was high at the beginning of the recording or when an individual entered into the recording room (Fig. 6). Therefore, it is the state of alertness, *per se*, and not the stimuli that increase gamma band coherence.

Gamma coherence during sleep

The intercortical dialogue during wakefulness and sleep has been analysed with standard EEG recordings in humans (Achermann & Borbely, 1998a,b), and an increase in gamma band (up to 50 Hz) coherence during REM sleep in comparison with NREM sleep was observed (Achermann & Borbely, 1998a,b). This effect was subtle and mainly present between anterior inter-hemispheric homologous leads. However, the preceding authors were cautious in interpreting their findings because of the low amplitude of high-frequency signals of the standard EEG recordings.

Nir *et al.* (2008) studied inter-hemispheric correlations of envelopes (0.1 Hz) of gamma oscillations during REM sleep and Stage 2 NREM sleep in comparison with wakefulness (Nir *et al.*, 2008). However, the coupling of gamma waves, *per se*, was not the focus of this study. In rats, Gervasoni *et al.* (2004) analysed pooled gamma (30–55 Hz) coherence between neocortical, hippocampal as well as subcortical loci (caudate-putamen and thalamus). They found that REM sleep was the state of maximum pooled coherence in the gamma range; however, gamma coherence among different neocortical sites was not analysed.

The results of the present study led to a different conclusion compared with the study of Llinas & Ribary (1993), who reported that during REM sleep magneto-EEG 40-Hz oscillations were similar in distribution, phase and amplitude to those observed during wakefulness; in contrast, gamma coherent activity was reduced during NREM sleep. They also found that gamma oscillations become robustly coherent in short time windows after sensory stimulation during waking; in other words, sensory stimuli 'reset' gamma oscillations. This effect was not observed during REM sleep. The preceding authors considered that dreams during REM sleep represent a state of hyper-attentiveness in which sensory inputs cannot address the processes that generate conscious experience (Llinas & Ribary, 1993). The discrepancies with our data may arise from the different analytical approaches; Llinas & Ribary (1993) analysed coherence by superimposing 37 traces (filtered at 35–45 Hz) recorded during 0.6–3-s epochs. It is likely that small time periods of high gamma coherence may appear in humans during phasic periods of REM sleep; in fact an increase in gamma activity was found during these periods (Gross & Gotman, 1999). However, we hypothesize that this increase in gamma coherence would not be maintained if larger periods of REM sleep (that include tonic REM sleep) were analysed.

In contrast to the references cited in the preceding paragraphs, several reports are in agreement with our results. Perez-Garci *et al.* (2001) reported that there is a decrease in correlation spectra in 2-s epochs of fast (27–48 Hz) frequencies restricted to intra-hemispheric frontal-perceptual cortical regions during REM sleep in humans (Perez-Garci *et al.*, 2001). However, among perceptual regions, correlation values for REM sleep and wakefulness were similar. Cantero *et al.* (2004) employed human intracranial EEG recordings for coherence analyses during sleep, which allow a much finer spatial scale than do scalp-recorded signals. They found that local (within neocortical regions) and long-range (between intra-hemispheric neocortical regions) gamma coherence was significantly greater during wakefulness than during sleep (Cantero *et al.*, 2004). However, no differences in coherence in the 35–58 Hz frequency band were found between NREM and REM sleep. Furthermore, functional gamma-range coupling between the neocortex and hippocampus was observed during wakefulness, but not during REM sleep. A recent study by Voss *et al.* (2009) demonstrated that coherence for all EEG spectra decreases during REM sleep compared with wakefulness (Voss *et al.*, 2009); interestingly, during lucid dreaming, coherence values are intermediate between wakefulness and REM sleep.

In the present paper, we have demonstrated in the cat that gamma intra-hemispheric coherence is practically absent during REM sleep. This was true for coherence measured between prefrontal and perceptual regions of the cortex, and among perceptual cortices, including primary as well as associative sensory areas. Interestingly, gamma band uncoupling during REM sleep was readily observed by simple inspection of filtered recordings. Future studies are needed to analyse the degree of gamma band coupling of cortical and subcortical areas that increase their activity during REM sleep, such as the limbic cortices and amygdala (Schwartz & Maquet, 2002).

Our demonstration that there is a radical reduction in gamma coherence during REM sleep between different and distant cortical

regions does not contradict findings from Steriade's group, which show an increase in local coupling (within a column or among closely cortical sites) during activated states (Steriade *et al.*, 1996; Destexhe *et al.*, 1999). In fact, as suggested in Figs 5 and 10, gamma power values (as a reflection of local gamma synchronization) during REM sleep were similar to QW and greater than during NREM sleep.

Absence of gamma coherence during REM sleep – impact on cognitive functions

A proper understanding of cognitive functions cannot be achieved without an understanding of consciousness, which involves a system's capacity to integrate information (Tononi, 2010). Recently, utilizing transcranial magnetic stimulation (TMS) and high-density EEG recordings in humans, Massimini *et al.* (2010) demonstrated that although during NREM sleep TMS elicited local and stereotypical cortical activations, during REM sleep TMS triggered a widespread and differentiated patterns of cortical activation that were similar to those observed during wakefulness. These data indicate that there is a significant impairment in intracortical dialogue during NREM sleep, although during REM sleep interactions among cortical sites are operative (Massimini *et al.*, 2010). However, in this study the frequency bands of the cortical interactions were not analysed. Our results in the cat and previous results from humans clearly show that, compared with wakefulness, during REM sleep there is a failure in the capacity of integration among different cortices, at least in high frequency ranges (Perez-Garci *et al.*, 2001; Cantero *et al.*, 2004; Voss *et al.*, 2009). This phenomenon may underlie some of the unique patterns of REM sleep mentation (Hobson, 2009; Nir & Tononi, 2010); in fact, the prevalence of thoughts decreases from wakefulness to NREM sleep and reach a nadir during REM sleep (the same as gamma coherence), while hallucinations and emotions follow an inverse pattern (Fosse *et al.*, 2001).

Bullock *et al.* (2003) considered that the following processes result in an increase in coherence between two structures: (1) both structures are driven by the same generator, (2) both structures can mutually drive each other and (3) one of the structures drives the other one. It is likely that differential activation of regulatory (cholinergic, monoaminergic and peptidergic) systems during REM sleep may be the foundation for cortical uncoupling (Watson *et al.*, 2010). Although it is not clear what role is played by these neuromodulatory systems with respect to large-scale cortical interactions, it is accepted that at least some of these systems alter the frequency range and the strength of local cortical oscillations (Munk *et al.*, 1996; Rodriguez *et al.*, 2004; Roopun *et al.*, 2010). Recent studies have demonstrated the presence of gamma activity in the reticular activating system (RAS), and have suggested that this activity helps to stabilize coherence related to arousal (reviewed by Urbano *et al.*, 2012); however, the role of gamma activity in the RAS during REM sleep is unknown. Nevertheless, the study of mechanisms that support the modification of gamma coherence during sleep and wakefulness was beyond the scope of the present report.

Conclusions

During REM sleep in the cat, despite an activated (desynchronized) EEG, there is an absence of cross-talk between different cortical regions in the gamma frequency band. Therefore, functional interactions among different cortical areas (re-entries), which are critical for cognitive functions, are different during wakefulness and REM sleep. This uncoupling of gamma frequency activity during REM sleep may be involved in the distinctiveness of the cognitive operations that take place during mentation that occur during wakefulness and REM sleep (dreams).

Acknowledgements

We thank Luciana Benedetto and Matias Cavelli for their technical assistance. We are also grateful to Dr Giancarlo Vanini for critical comments regarding the manuscript. We are indebted to several anonymous reviewers for comments on the manuscript. The 'Programa de Desarrollo de Ciencias Básicas' (PEDECIBA), Uruguay, partially supported this work.

Conflict of interest

None.

References

Achermann, P. & Borbely, A.A. (1998a) Coherence analysis of the human sleep electroencephalogram. *Neuroscience*, **85**, 1195–1208.

Achermann, P. & Borbely, A.A. (1998b) Temporal evolution of coherence and power in the human sleep electroencephalogram. *J. Sleep Res.*, **7**(Suppl. 1), 36–41.

Berman, A.L. & Jones, E.G. (1982). *The Thalamus and Basal Telencephalum of the Cat. A Citoarchitectonic Atlas with Stereotaxic Coordinates*. University of Wisconsin, Madison.

Bouyer, J.J., Montaron, M.F. & Rougeul, A. (1981) Fast fronto-parietal rhythms during combined focused attentive behaviour and immobility in cat: cortical and thalamic localizations. *Electroencephalogr. Clin. Neurophysiol.*, **51**, 244–252.

Bressler, S.L., Coppola, R. & Nakamura, R. (1993) Episodic multiregional cortical coherence at multiple frequencies during visual task performance. *Nature*, **366**, 153–156.

Bullock, T.H. (1997) Signals and signs in the nervous system: the dynamic anatomy of electrical activity is probably information-rich. *Proc. Natl Acad. Sci. USA*, **94**, 1–6.

Bullock, T.H. & McClune, M.C. (1989) Lateral coherence of the electrocorticogram: a new measure of brain synchrony. *Electroencephalogr. Clin. Neurophysiol.*, **73**, 479–498.

Bullock, T.H., McClune, M.C., Achimowicz, J.Z., Iragui-Madoz, V.J., Duckrow, R.B. & Spencer, S.S. (1995a) EEG coherence has structure in the millimeter domain: subdural and hippocampal recordings from epileptic patients. *Electroencephalogr. Clin. Neurophysiol.*, **95**, 161–177.

Bullock, T.H., McClune, M.C., Achimowicz, J.Z., Iragui-Madoz, V.J., Duckrow, R.B. & Spencer, S.S. (1995b) Temporal fluctuations in coherence of brain waves. *Proc. Natl Acad. Sci. USA*, **92**, 11568–11572.

Bullock, T.H., McClune, M.C. & Enright, J.T. (2003) Are the electroencephalograms mainly rhythmic? Assessment of periodicity in wide-band time series. *Neuroscience*, **121**, 233–252.

Buzsaki, G. & Wang, X.J. (2012) Mechanisms of gamma oscillations. *Annu. Rev. Neurosci.*, **35**, 203–225.

Cantero, J.L., Atienza, M. & Salas, R.M. (2000) Clinical value of EEG coherence as electrophysiological index of cortico-cortical connections during sleep. *Rev. Neurol.*, **31**, 442–454.

Cantero, J.L., Atienza, M., Madsen, J.R. & Stickgold, R. (2004) Gamma EEG dynamics in neocortex and hippocampus during human wakefulness and sleep. *Neuroimage*, **22**, 1271–1280.

Castro, S., Benedetto, L., Gutierrez, M., Falconi, A. & Torterolo, P. (2010) 'Coherence' in the cortical electrical activity during sleep and wakefulness. In *3rd International Congress on Sleep Medicine and 12th Brazilian Congress on Sleep Medicine*. San Pablo.

Castro, S., Gutierrez, M., Falconi, A., Chase, M. & Torterolo, P. (2011) Absence of EEG gamma (35-40 Hz) coherence characterizes REM sleep and differentiates it from wakefulness. In *41st Annual Meeting of the Society for Neuroscience*. Washington.

Corsi-Cabrera, M., Miro, E., del-Rio-Portilla, Y., Perez-Garci, E., Villanueva, Y. & Guevara, M.A. (2003) Rapid eye movement sleep dreaming is characterized by uncoupled EEG activity between frontal and perceptual cortical regions. *Brain Cogn.*, **51**, 337–345.

Das, N.N. & Gastaut, H. (1955) Variations de l'activite electrique du cerveau, du coeur et des muscles squellettiques au cours de la meditation et de l'extase yoguique. *Electroencephalogr. Clin. Neurophysiol.*, **6**, 211.

Destexhe, A., Contreras, D. & Steriade, M. (1999) Spatiotemporal analysis of local field potentials and unit discharges in cat cerebral cortex during natural wake and sleep states. *J. Neurosci.*, **19**, 4595–4608.
Edelman, G.M. & Tononi, G. (2000). *A Universe of Consciousness*. Basic Books, New York.
Fosse, R., Stickgold, R. & Hobson, J.A. (2001) Brain-mind states: reciprocal variation in thoughts and hallucinations. *Psychol. Sci.*, **12**, 30–36.
Fuster, J.M. (1989). *The Prefrontal Cortex*. Raven Press, New York.
Gervasoni, D., Lin, S.C., Ribeiro, S., Soares, E.S., Pantoja, J. & Nicolelis, M.A. (2004) Global forebrain dynamics predict rat behavioral states and their transitions. *J. Neurosci.*, **24**, 11137–11147.
Gross, D.W. & Gotman, J. (1999) Correlation of high-frequency oscillations with the sleep–wake cycle and cognitive activity in humans. *Neuroscience*, **94**, 1005–1018.
Harle, M., Rockstroh, B.S., Keil, A., Wienbruch, C. & Elbert, T.R. (2004) Mapping the brain's orchestration during speech comprehension: task-specific facilitation of regional synchrony in neural networks. *BMC Neurosci.*, **5**, 40.
Hobson, J.A. (2009) REM sleep and dreaming: towards a theory of protoconsciousness. *Nat. Rev. Neurosci.*, **10**, 803–813.
Jasper, H.H. & Andrews, H.L. (1938) Brain potentials and voluntary muscle activity in man. *J. Neurophysiol.*, **1**, 87–100.
John, E.R. (2002) The neurophysics of consciousness. *Brain Res. Brain Res. Rev.*, **39**, 1–28.
Libet, B., Pearl, D.K., Morledge, D.E., Gleason, C.A., Hosobuchi, Y. & Barbaro, N.M. (1991) Control of the transition from sensory detection to sensory awareness in man by the duration of a thalamic stimulus. The cerebral 'time-on' factor. *Brain*, **114**, 1731–1757.
Llinas, R. & Ribary, U. (1993) Coherent 40-Hz oscillation characterizes dream state in humans. *Proc. Natl Acad. Sci. USA*, **90**, 2078–2081.
Llinas, R., Ribary, U., Contreras, D. & Pedroarena, C. (1998) The neuronal basis for consciousness. *Philos. Trans. R. Soc. Lond. B Biol. Sci.*, **353**, 1841–1849.
Maloney, K.J., Cape, E.G., Gotman, J. & Jones, B.E. (1997) High-frequency gamma electroencephalogram activity in association with sleep-wake states and spontaneous behaviors in the rat. *Neuroscience*, **76**, 541–555.
von der Malsburg, C. (1995) Binding in models of perception and brain function. *Curr. Opin. Neurobiol.*, **5**, 520–526.
Markowitsch, H.J. & Pritzel, M. (1977) A stereotaxic atlas of the prefrontal cortex of the cat. *Acta Neurobiol. Exp. (Wars)*, **37**, 63–81.
Mashour, G.A. (2006) Integrating the science of consciousness and anesthesia. *Anesth. Analg.*, **103**, 975–982.
Massimini, M., Ferrarelli, F., Murphy, M., Huber, R., Riedner, B., Casarotto, S. & Tononi, G. (2010) Cortical reactivity and effective connectivity during REM sleep in humans. *Cogn. Neurosci.*, **1**, 176–183.
Morrison, A.R. (1983) A window on the sleeping brain. *Sci. Am.*, **248**, 94–102.
Munk, M.H., Roelfsema, P.R., Konig, P., Engel, A.K. & Singer, W. (1996) Role of reticular activation in the modulation of intracortical synchronization. *Science*, **272**, 271–274.
Nir, Y. & Tononi, G. (2010) Dreaming and the brain: from phenomenology to neurophysiology. *Trends Cogn. Sci.*, **14**, 88–100.
Nir, Y., Mukamel, R., Dinstein, I., Privman, E., Harel, M., Fisch, L., Gelbard-Sagiv, H., Kipervasser, S., Andelman, F., Neufeld, M.Y., Kramer, U., Arieli, A., Fried, I. & Malach, R. (2008) Interhemispheric correlations of slow spontaneous neuronal fluctuations revealed in human sensory cortex. *Nat. Neurosci.*, **11**, 1100–1108.
Nunez, P.L., Srinivasan, R., Westdorp, A.F., Wijesinghe, R.S., Tucker, D.M., Silberstein, R.B. & Cadusch, P.J. (1997) EEG coherency. I: statistics, reference electrode, volume conduction, Laplacians, cortical imaging, and interpretation at multiple scales. *Electroencephalogr. Clin. Neurophysiol.*, **103**, 499–515.
Perez-Garci, E., del-Rio-Portilla, Y., Guevara, M.A., Arce, C. & Corsi-Cabrera, M. (2001) Paradoxical sleep is characterized by uncoupled gamma activity between frontal and perceptual cortical regions. *Sleep*, **24**, 118–126.
Rechtschaffen, A. (1978) The single-mindedness and isolation of dreams. *Sleep*, **1**, 97–109.
Rieder, M.K., Rahm, B., Williams, J.D. & Kaiser, J. (2010) Human gamma-band activity and behavior. *Int. J. Psychophysiol.*, **79**, 39–48.
Rodriguez, R., Kallenbach, U., Singer, W. & Munk, M.H. (2004) Short- and long-term effects of cholinergic modulation on gamma oscillations and response synchronization in the visual cortex. *J. Neurosci.*, **24**, 10369–10378.
Roopun, A.K., Lebeau, F.E., Ramell, J., Cunningham, M.O., Traub, R.D. & Whittington, M.A. (2010) Cholinergic neuromodulation controls directed temporal communication in neocortex in vitro. *Front. Neural Circuits*, **4**, 8.
Sastre, J.P. & Jouvet, M. (1979) Oneiric behavior in cats. *Physiol. Behav.*, **22**, 979–989.
Scannell, J.W., Blakemore, C. & Young, M.P. (1995) Analysis of connectivity in the cat cerebral cortex. *J. Neurosci.*, **15**, 1463–1483.
Schwartz, S. & Maquet, P. (2002) Sleep imaging and the neuro-psychological assessment of dreams. *Trends Cogn. Sci.*, **6**, 23–30.
Siegel, M., Donner, T.H. & Engel, A.K. (2012) Spectral fingerprints of large-scale neuronal interactions. *Nat. Rev. Neurosci.*, **13**, 121–134.
Steriade, M., Amzica, F. & Contreras, D. (1996) Synchronization of fast (30–40 Hz) spontaneous cortical rhythms during brain activation. *J. Neurosci.*, **16**, 392–417.
Thompson, R.F., Johnson, R.H. & Hoopes, J.J. (1963) Organization of auditory, somatic sensory, and visual projection to association fields of cerebral cortex in the cat. *J. Neurophysiol.*, **26**, 343–364.
Tiitinen, H., Sinkkonen, J., Reinikainen, K., Alho, K., Lavikainen, J. & Naatanen, R. (1993) Selective attention enhances the auditory 40-Hz transient response in humans. *Nature*, **364**, 59–60.
Tononi, G. (2010) Information integration: its relevance to brain function and consciousness. *Arch. Ital. Biol.*, **148**, 299–322.
Torterolo, P., Morales, F.R. & Chase, M.H. (2002) GABAergic mechanisms in the pedunculopontine tegmental nucleus of the cat promote active (REM) sleep. *Brain Res.*, **944**, 1–9.
Torterolo, P., Yamuy, J., Sampogna, S., Morales, F.R. & Chase, M.H. (2003) Hypocretinergic neurons are primarily involved in activation of the somatomotor system. *Sleep*, **1**, 25–28.
Torterolo, P., Benedetto, L., Lagos, P., Sampogna, S. & Chase, M.H. (2009) State-dependent pattern of Fos protein expression in regionally-specific sites within the preoptic area of the cat. *Brain Res.*, **1267**, 44–56.
Torterolo, P., Ramos, O.V., Sampogna, S. & Chase, M.H. (2011a) Hypocretinergic neurons are activated in conjunction with goal-oriented survival-related motor behaviors. *Physiol. Behav.*, **104**, 823–830.
Torterolo, P., Sampogna, S. & Chase, M.H. (2011b) A restricted parabrachial pontine region is active during non-rapid eye movement sleep. *Neuroscience*, **190**, 184–193.
Uhlhaas, P.J., Pipa, G., Lima, B., Melloni, L., Neuenschwander, S., Nikolic, D. & Singer, W. (2009) Neural synchrony in cortical networks: history, concept and current status. *Front. Integr. Neurosci.*, **3**, 17.
Uhlhaas, P.J., Pipa, G., Neuenschwander, S., Wibral, M. & Singer, W. (2011) A new look at gamma? High- (>60 Hz) gamma-band activity in cortical networks: function, mechanisms and impairment. *Prog. Biophys. Mol. Biol.*, **105**, 14–28.
Urbano, F.J., Kezunovic, N., Hyde, J., Simon, C., Beck, P. & Garcia-Rill, E. (2012) Gamma band activity in the reticular activating system. *Front. Neurol.*, **3**, 6.
Ursin, R. & Sterman, M. (1981). *Manual for Standardized Scoring of Sleep and Waking States in Adult Cats*. BIS/BRI, University of California, Los Angeles.
Velik, R. (2009) From single neuron-firing to consciousness – towards the true solution of the binding problem. *Neurosci. Biobehav. Rev.*, **34**, 993–1001.
Voss, U., Holzmann, R., Tuin, I. & Hobson, J.A. (2009) Lucid dreaming: a state of consciousness with features of both waking and non-lucid dreaming. *Sleep*, **32**, 1191–1200.
Watson, C., Baghdoyan, H. & Lydic, R. (2010). A neurochemical perspective on states of consciousness. In Hudetz, A.G. & Pearce, R. (Eds), *Supressing the Mind, Contemporary Clinical Neuroscience*. Humana Press, New York, pp. 33–79.
Yuval-Greenberg, S., Tomer, O., Keren, A.S., Nelken, I. & Deouell, L.Y. (2008) Transient induced gamma-band response in EEG as a manifestation of miniature saccades. *Neuron*, **58**, 429–441.

Graphical Abstract

The contents of this page will be used as part of the graphical abstract of html only. It will not be published as part of main article.

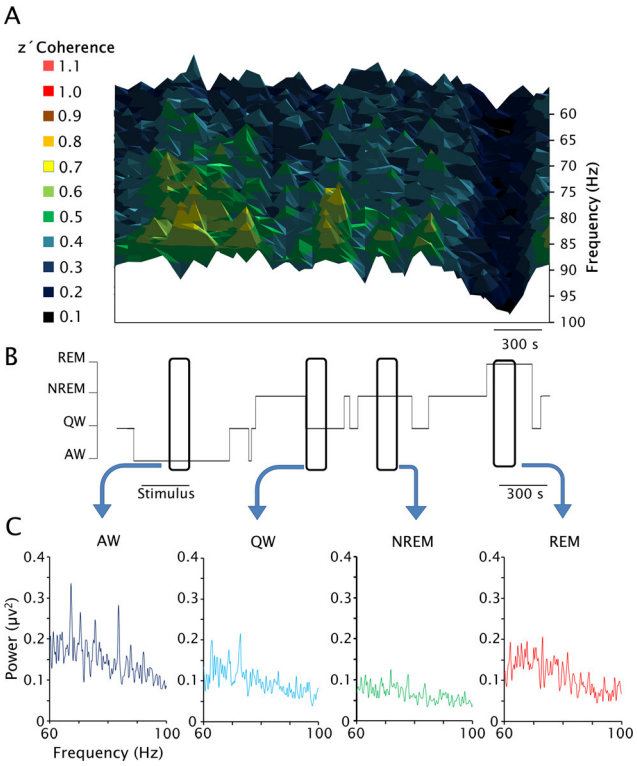

During cognitive processes there are extensive interactions between various regions of the cerebral cortex. Oscillations in the gamma frequency band ($\approx$ 40 Hz) of the elecroencephalogram (EEG) are involved in the binding of spatially separated but temporally correlated neural events, which results in a unified perceptual experience.

Author Query Form

Journal: EJN

Article: 12143

Dear Author,
During the copy-editing of your paper, the following queries arose. Please respond to these by marking up your proofs with the necessary changes/additions. Please write your answers on the query sheet if there is insufficient space on the page proofs. Please write clearly and follow the conventions shown on the attached corrections sheet. If returning the proof by fax do not write too close to the paper's edge. Please remember that illegible mark-ups may delay publication.

Many thanks for your assistance.

Query reference	Query	Remarks
1	**AUTHOR: Please check that authors and their affiliations are correct.**	
2	**AUTHOR: Please abbreviaton list if applicable.**	

WILEY-BLACKWELL

USING e-ANNOTATION TOOLS FOR ELECTRONIC PROOF CORRECTION

Required software to e-Annotate PDFs: Adobe Acrobat Professional or Adobe Reader (version 7.0 or above). (Note that this document uses screenshots from Adobe Reader X)
The latest version of Acrobat Reader can be downloaded for free at: http://get.adobe.com/uk/reader/

Once you have Acrobat Reader open on your computer, click on the Comment tab at the right of the toolbar:

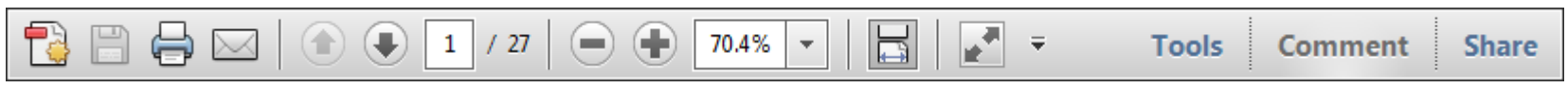

This will open up a panel down the right side of the document. The majority of tools you will use for annotating your proof will be in the Annotations section, pictured opposite. We've picked out some of these tools below:

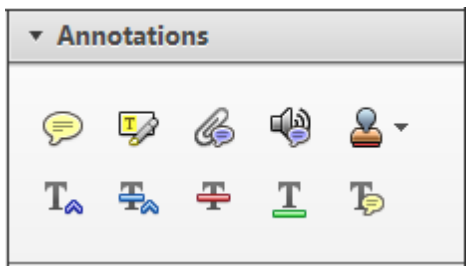

1. Replace (Ins) Tool – for replacing text.

Strikes a line through text and opens up a text box where replacement text can be entered.

How to use it

- Highlight a word or sentence.
- Click on the Replace (Ins) icon in the Annotations section.
- Type the replacement text into the blue box that appears.

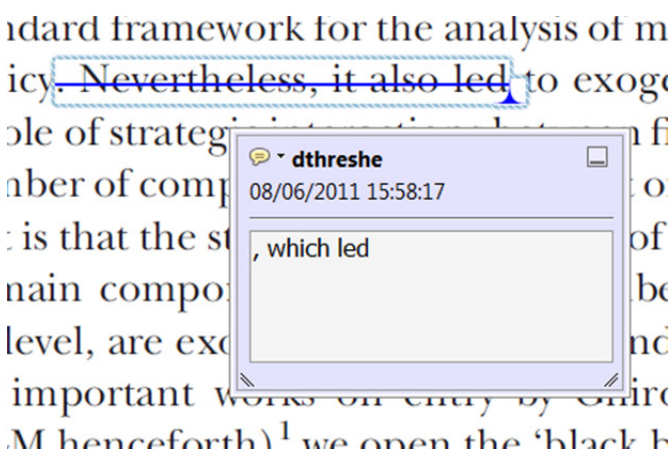

2. Strikethrough (Del) Tool – for deleting text.

Strikes a red line through text that is to be deleted.

How to use it

- Highlight a word or sentence.
- Click on the Strikethrough (Del) icon in the Annotations section.

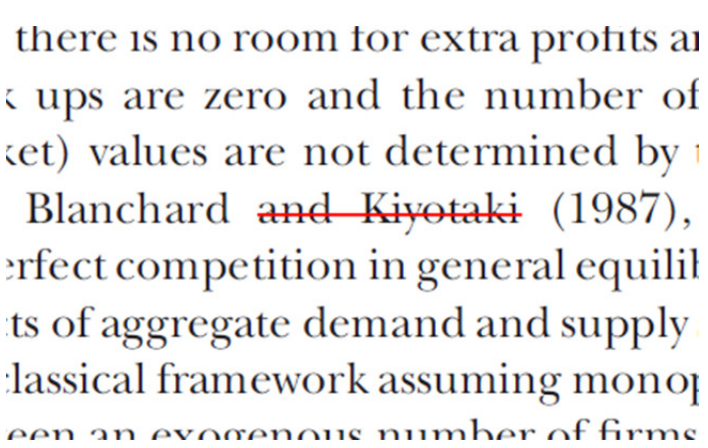

3. Add note to text Tool – for highlighting a section to be changed to bold or italic.

Highlights text in yellow and opens up a text box where comments can be entered.

How to use it

- Highlight the relevant section of text.
- Click on the Add note to text icon in the Annotations section.
- Type instruction on what should be changed regarding the text into the yellow box that appears.

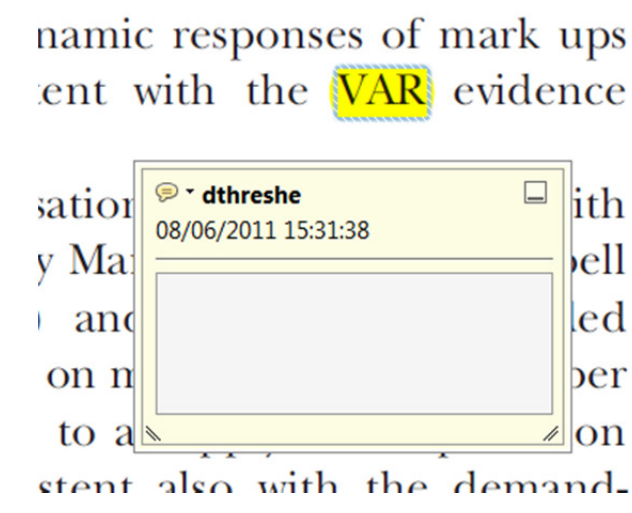

4. Add sticky note Tool – for making notes at specific points in the text.

Marks a point in the proof where a comment needs to be highlighted.

How to use it

- Click on the Add sticky note icon in the Annotations section.
- Click at the point in the proof where the comment should be inserted.
- Type the comment into the yellow box that appears.

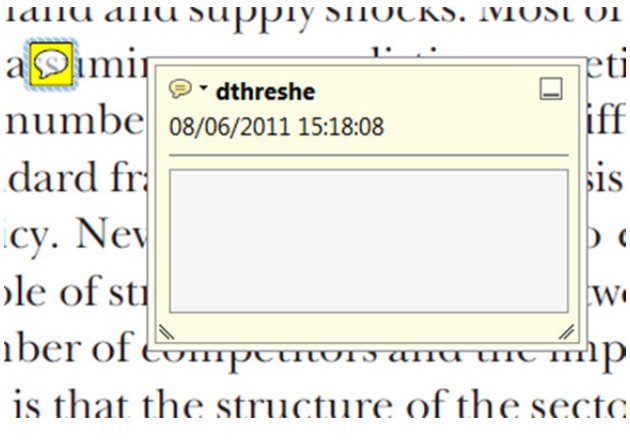

WILEY-BLACKWELL

USING e-ANNOTATION TOOLS FOR ELECTRONIC PROOF CORRECTION

5. Attach File Tool – for inserting large amounts of text or replacement figures.

Inserts an icon linking to the attached file in the appropriate pace in the text.

How to use it

- Click on the Attach File icon in the Annotations section.
- Click on the proof to where you'd like the attached file to be linked.
- Select the file to be attached from your computer or network.
- Select the colour and type of icon that will appear in the proof. Click OK.

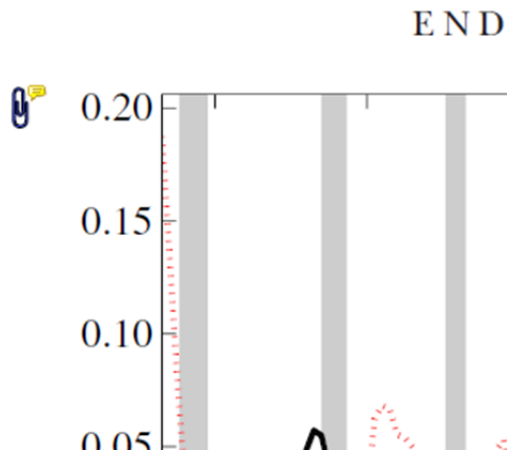

6. Add stamp Tool – for approving a proof if no corrections are required.

Inserts a selected stamp onto an appropriate place in the proof.

How to use it

- Click on the Add stamp icon in the Annotations section.
- Select the stamp you want to use. (The Approved stamp is usually available directly in the menu that appears).
- Click on the proof where you'd like the stamp to appear. (Where a proof is to be approved as it is, this would normally be on the first page).

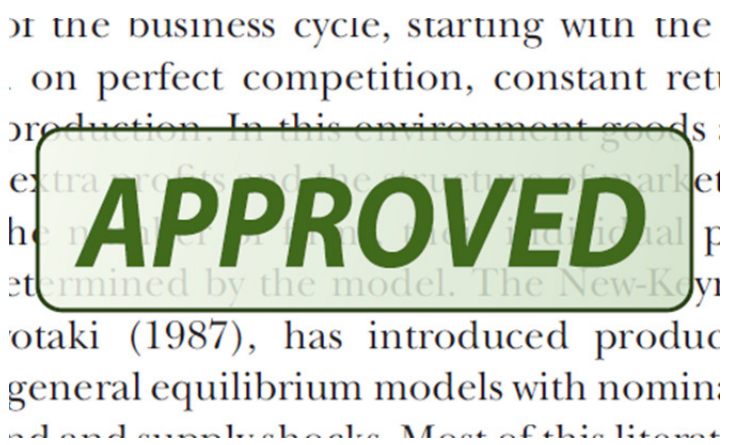

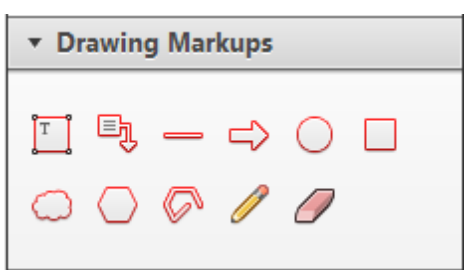

7. Drawing Markups Tools – for drawing shapes, lines and freeform annotations on proofs and commenting on these marks.

Allows shapes, lines and freeform annotations to be drawn on proofs and for comment to be made on these marks..

How to use it

- Click on one of the shapes in the Drawing Markups section.
- Click on the proof at the relevant point and draw the selected shape with the cursor.
- To add a comment to the drawn shape, move the cursor over the shape until an arrowhead appears.
- Double click on the shape and type any text in the red box that appears.

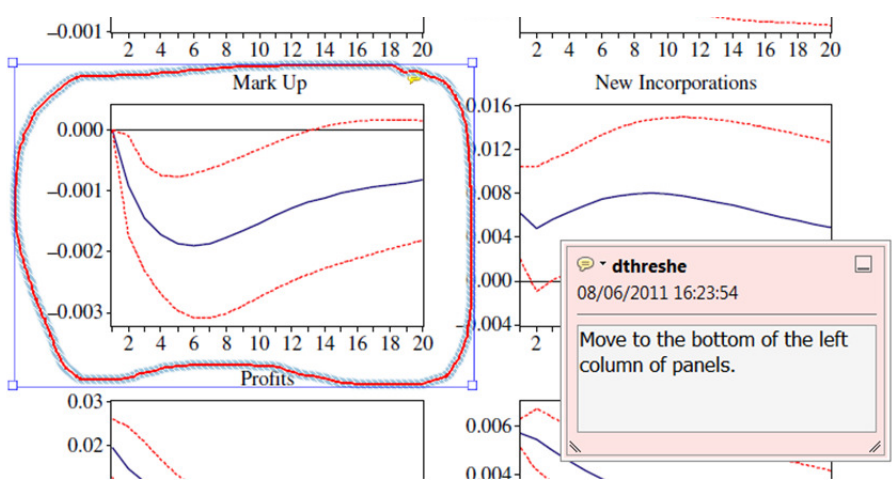

For further information on how to annotate proofs, click on the Help menu to reveal a list of further options: